Title: Mutagenesis Induced by Protonation of Single-Stranded DNA is Linked to Glycolytic Sugar Metabolism

Short Title: Mutagenesis Induced by Protonation of Single-Stranded DNA

Authors: Suzana P. Gelova and Kin Chan*

* Corresponding Author: kin.chan@uottawa.ca

Affiliations:

Department of Biochemistry, Microbiology and Immunology

Ottawa Institute of Systems Biology

University of Ottawa, Ottawa, Ontario, Canada

Abstract

Mutagenesis can be thought of as random, in the sense that the occurrence of each mutational event cannot be predicted with precision in space or time. However, when sufficiently large numbers of mutations are analyzed, recurrent patterns of base changes called mutational signatures can be detected. To date, some 60 single base substitution or SBS signatures have been derived from analysis of cancer genomics data. We recently reported that the ubiquitous signature SBS5 matches the pattern of single nucleotide polymorphisms (SNPs) in humans and has analogs in many species. Using a temperature-sensitive single-stranded DNA mutation reporter system, we also showed that a similar mutational pattern in yeast is dependent on translesion DNA synthesis and glycolytic sugar metabolism. Here, we investigated mechanisms that are responsible for the SBS5-like mutagenesis in yeast. We first confirmed that excess sugar metabolism leads to increased mutation rate, which was detectable by fluctuation assay. We then ruled out a role for aerobic respiration in SBS5-like mutagenesis by observing that petite and wild-type cells did not exhibit statistical differences in mutation frequencies. Since glycolysis is known to produce excess protons, we then investigated the effects of experimental manipulations on pH and mutagenesis. We hypothesized that yeast metabolizing 8% glucose would produce more excess protons than cells in 2% glucose. Consistent with this, cells metabolizing 8% glucose had lower intracellular and extracellular pH values. Similarly, deletion of *vma3* (encoding a vacuolar H^+-ATPase subunit) increased mutagenesis. We also found that treating cells with edelfosine (which renders membranes more permeable, including to protons) or culturing in low pH media increased mutagenesis. Altogether, our results agree with multiple biochemical studies

showing that protonation of nitrogenous bases can alter base pairing, and shed new light on a ubiquitous form of intrinsic mutagenesis in many biological contexts.

Introduction

Mutations can be the starting material for evolution by natural selection. Mutations oftentimes result after DNA damage from either endogenous processes (1) or exogenous exposures (2–4). Endogenous DNA damaging processes include the following: deamination of cytosine or 5-methylcytosine to uracil or thymine, respectively (5–9); base oxidation (10,11); base alkylation (5,12,13); glycosidic bond breakage (5,14–16); and single- and double-stranded DNA breaks (5,17,18). Exogenous DNA damage can take on many forms, including: aflatoxin (19); aristolochic acid (20); ionizing radiation (4); tobacco (21); and ultraviolet (UV) light (3). Spontaneous ionization or isomerization (i.e., tautomerization) of DNA bases can also alter base pairing characteristics and are thought to be another possible source of mutations (22–25).

It is important to note that these and other processes/exposures, which damage DNA, do not affect all bases equally. Adenine, cytosine, guanine, and thymine in DNA each have their own specific set of reactive chemical groups (i.e., amines, carbonyls, ring atoms) (26). The local sequence context can also be a key factor affecting susceptibility to DNA damage. As a result, any given DNA damaging process or agent may be more likely to react with some base(s) than others, yielding recurrent, reproducible patterns of sequence changes that have been termed mutational signatures (27).

Mutational signatures typically are extracted from genomic data sets using the non-negative matrix factorization (NMF) algorithm (28). There are approximately 60 single base substitution (SBS) signatures described in the Catalog of Somatic Mutations in Cancer (or COSMIC) at this point (29). Many mutational signatures have well-defined

etiologies, such as: SBS1 from deamination of 5-methylcytosine at CpG motifs; SBS2 and SBS13 from enzymatic deamination of cytosine at TC motifs by APOBEC deaminases; SBS3 from deficiencies in homologous recombination DNA repair; SBS4 and SBS29 from tobacco smoking and chewing, respectively; SBS6, SBS15, SBS21, SBS26, and SBS44 from various deficiencies in DNA mismatch repair; SBS7a through SBS7d from ultraviolet light exposure; SBS10a through SBS10d from mutation of the replicative DNA polymerases epsilon or delta; SBS18 from reactive oxygen species; and SBS30 and SBS36 from DNA base excision repair deficiencies (27). Currently, about one-third of the previously described mutational signatures remain of undefined etiology (29). Further, with more sequencing data being produced on a continuing basis, more mutational signatures surely remain to be discovered as well.

In spite of the great deal of progress made to elucidate the etiologies of mutational signatures, one of the most common remains relatively poorly understood. This signature, SBS5. is found in all cancer types and is present in almost all individual cancer samples, being typically one of the most prominent signatures in each sample (27). The numbers of mutations attributed to SBS5 increase steadily as we age; interestingly, there is considerable variation in the extent of this "clock-like" mutation accumulation effect between individuals, i.e., some have many SBS5 mutations while others have relatively few (30). Furthermore, over 70% of mutations in early human embryos (31) and ~75% of de novo mutations in human children (32) fit the SBS5 pattern. In contrast to other mutational signatures which can diminish in prevalence as cancers undergo subclonal diversification, SBS5 usually remains a prominent signature that contributes significantly to intratumor heterogeneity (33).

Previously, we showed that SBS5 is the human counterpart in a continuum of similar intrinsic mutational patterns in many species. Indeed, the pattern of human single nucleotide polymorphisms (SNPs) also matched SBS5 very closely (34). Additionally, we showed that a similar mutational pattern can be recapitulated using a baker's yeast (*Saccharomyces cerevisiae*) reporter system featuring controlled generation of genomic single-stranded DNA (ssDNA), by taking advantage of the *cdc13-1* point mutation, which triggers telomere uncapping and end resection upon temperature shifting (35). The SBS5-like mutational pattern was dependent on error-prone translesion DNA synthesis and sugar metabolism. More SBS5-like mutagenesis was observed when *cdc13-1* cells were arrested in G_2 in media with more glucose. Further, we showed that blocking the completion of glycolysis using a degron allele of the principle pyruvate kinase gene abrogated 90% of the SBS5-like mutagenesis (34).

In this work, we investigated mechanisms underlying this form of mutagenesis further. Our results show that excess sugar metabolism, in addition to increasing mutagenesis, has important effects on lowering both intracellular and extracellular pH. Moreover, our findings implicate protonation of ssDNA as a likely source of the increased mutagenesis. Our study provides fresh insights on the molecular underpinnings of a ubiquitous type of mutagenesis observed in many biological systems.

Results

Increased glucose metabolism leads to increased mutagenesis

Mutation frequency experiments were done using haploid yeast strains (ySR127, the parental strain, and its derivatives) that form long stretches of sub-telomeric single-stranded DNA (ssDNA) when shifted to 37°C, due to the *cdc13-1* temperature-sensitive point mutation (36) (see Figure 1A). At 37°C the mutant cdc13-1 protein dissociates from telomeres, leaving the unprotected chromosome ends vulnerable to enzymatic resection. Once significant resection does occur, the DNA damage checkpoint is activated to arrest cells in the G_2 phase of the cell cycle (36). Three reporter genes (*CAN1*, *ADE2*, and *URA3*) had been deleted from their native loci and repositioned to the left sub-telomeric region of chromosome V (35). This mutagenesis system is exceptionally well suited to investigating weak mutagens or subtle mutagenic effects, since the ssDNA is more prone to mutation than double-stranded DNA (dsDNA) and high-fidelity repair using the complementary strand would not be possible. The ssDNA system has been used previously to elucidate the mutagenic effects of bisulfite and human APOBEC3G cytidine deaminase (35); abasic sites (37); reactive oxygen species (38); human APOBEC3A and APOBEC3B cytidine deaminases (39); as well as alkylating agents (40).

We began by comparing the mutagenic effects of metabolizing rich media with either 2% vs. 8% glucose. When ySR127 cells were grown at 23°C, there was no statistical difference in frequency of *CAN1* gene inactivation between 2% vs. 8% glucose (paired t-test P-value = 0.0858, see Figure 1B). The sub-telomeric DNA at permissive

temperature should have remained canonically double-stranded, so it should be better protected from mutagenesis. In contrast, when cells were shifted to 37°C, resulting in exposure of sub-telomeric ssDNA, there was a clearly detectable difference in mutagenesis when metabolizing 2% vs. 8% glucose (paired t-test P-value = 0.00166, see Figure 1B). These results reaffirm previous observations (41).

We then ran additional experiments to check if the excess osmolarity in media with 8% glucose might affect mutagenesis. To do this, we compared mutation frequencies when metabolizing media with 2% glucose vs. 2% glucose + 6% sorbitol vs. 8% glucose. At 23°C, we did not observe a statistically significant effect on mutagenesis due to differences in media (ANOVA P-value = 0.0726, see Figure 1C). But at 37°C, we did find a significant effect on mutagenesis among the different media (ANOVA P-value = 1.74×10^{-7}, see Figure 1C). To determine which media were statistically different from each other, we then ran the Tukey Honest Statistical Differences (HSD) test, and determined that at 37°C, the cells in 8% glucose media had higher mutation frequencies than cells in the other two media types (see Table 2). Cells metabolizing 2% glucose media did not have statistically different mutation frequencies than cells metabolizing 2% glucose + 6% sorbitol media (see Table 2). From these results, we infer that the increase in mutation frequency when metabolizing 8% glucose was not likely due to increased osmolarity in the media.

We noticed that the mutation frequency results at 23°C came close to statistical significance when comparing 2% vs. 8% glucose. To determine if longer term metabolism could reveal differences in mutagenesis, we carried out fluctuation assays to determine mutation rates at permissive temperature (42). For ySR127, which has *cdc13-*

1 and the *CAN1-URA3-ADE2* reporter cassette near a chromosome end, we obtained mutation rates of 2.57×10^{-6} and 6.60×10^{-6} on 2% and 8% glucose media, respectively (flan.test parametric test P-value = 1.42×10^{-12}), indicating a clear difference. For ySR128, which is *CDC13*$^{+}$ and has the triple reporter gene cassette in a locus in the middle of chromosome II, we found mutation rates of 1.35×10^{-6} on 2% glucose media and 1.80×10^{-6} on 8% glucose (flan.test parametric P-value = 0.0111). As an additional control, we tested strain yKC023, which has *cdc13-1*, but the *CAN1-URA3-ADE2* reporter cassette is situated at the mid-chromosome II locus. For yKC023, we determined mutation rates of 2.34×10^{-6} and 2.48×10^{-6} on 2% and 8% glucose, respectively (flan.test parametric P-value = 0.648). We also tested yKC005, which is *CDC13*$^{+}$ but has the reporter gene cassette in the chromosome V sub-telomeric location. yKC005 yielded mutation rates of 8.93×10^{-7} on 2% glucose and 9.34×10^{-7} on 8% glucose (flan.test parametric P-value = 0.804). These data are summarized in Table 3. Consistent with the model that the SBS5-like mutagenesis in yeast is associated with ssDNA, these data showed the clearest difference in mutation rates for ySR127, which had the reporter cassette near a chromosome end and a mutation that destabilized the telomere capping complex.

<u>Aerobic respiration does not contribute to mutagenesis</u>

We noted previously that blocking the last step of glycolysis using a degron allele of *CDC19,* the pyruvate kinase gene expressed while metabolizing glucose (43), resulted in a 90% decrease in mutagenesis (34). Similarly, petite cells (lacking functional mitochondria) metabolizing 2% glucose did not exhibit any change in mutation frequency

(34). To investigate the possible role of aerobic respiration on SBS5-like mutagenesis further, we tested spontaneously occurring ρ^- and ethidium-induced ρ^0 cells, metabolizing media with either 2% or 8% glucose, at 23°C or shifted to 37°C for six hours. There was no statistically significant effect due to mitochondrial status (ANOVA P-value = 0.187), but as expected, there was a strong effect due to temperature shifting (ANOVA P-value = 1.55×10^{-17}, see Figure 2A). These results showed that the mutation frequencies did not depend on mitochondrial function, reaffirming a key role for glycolysis instead.

Media acidification from metabolizing more glucose

In glycolysis, decarboxylation of pyruvate produces carbon dioxide (CO_2) (44), which is rapidly hydrated by carbonic anhydrases to yield carbonic acid (H_2CO_3), so the net result is intracellular acidification (45). We reasoned that if cells metabolized more glucose, then more excess protons would have to be extruded out of the cells and into the media. This should result in a readily detectable decrease of extracellular pH in the conditioned media. We measured the pH of conditioned media for cells at 23°C or 37°C, metabolizing either 2% or 8% glucose. There was no statistical difference when comparing among the ρ status of the three genotypes (ANOVA P-value = 0.78), but there were significant differences due to treatment conditions (see Figure 2B and Table 4). There were statistically significant differences for the following pairwise comparisons of treatment conditions by the Tukey HSD test: 2% vs. 8% glucose at 23°C; 2% vs. 8% glucose at 37°C; and 23°C vs. 37°C in 2% glucose. Interestingly, there was no statistical difference for the 23°C vs. 37°C comparison in 8% glucose (Tukey HSD adjusted P-value = 0.965). Media pH was quite acidic when cells were metabolizing 8% glucose

(external pH $\lesssim$ 5), regardless of other factors, i.e., either genotype or temperature. This likely reflected the necessity for all the cells to put out a higher concentration of excess protons into the media when metabolizing the higher concentration of glucose.

Effect of extracellular pH on mutagenesis

We found previously that more glucose metabolism led to more mutagenesis, and have just noted that more glucose metabolism resulted in significantly more extracellular acidification. So, we next investigated if it might be possible to impinge on mutation frequency indirectly by controlling the extracellular pH. We shifted ySR127 cells to 37°C in either 2% or 8% glucose media adjusted to either pH 4, 5, 6, or 7 (see Figure 2C). ANOVA revealed a strong effect for glucose concentration on mutation frequency (P-value = 7.38×10^{-16}), as well as a significant effect for extracellular pH (P-value = 0.00823). Using the Tukey HSD test, we found that mutation frequencies in pH 4 and 5 media both were significantly higher than in pH 7 media (see Table 5). These data show that, with a sufficiently sensitive mutation detection system, it was actually possible to observe differences in induced mutagenesis due to manipulating extracellular pH.

Cells metabolizing more glucose have lower intracellular pH

Given that the extracellular pH values when cells metabolize 8% glucose media were lower than cells metabolizing 2% glucose, we reasoned that it might be possible to detect differences in intracellular pH as well. To test this, we expressed a pH-sensitive superfolder pHluorin variant of GFP (46) in the ySR127 background. The distribution of intracellular pH values for cells at 23°C in 8% glucose were statistically lower than for

cells in 2% glucose (paired t-test P-value = 0.0191, see Figure 3A). Similarly at 37°C, cells metabolizing 8% glucose had statistically lower intracellular pH value distributions than cells metabolizing 2% glucose (paired t-test P-value = 0.000742, see Figure 3B). These measurements show that, despite the action of homeostatic mechanisms to maintain intracellular pH within a narrow range (47), it was possible to detect differences when cells were metabolizing different concentrations of glucose glycolytically, as this metabolism would itself be the source for the excess protons. This detection was made possible using a sufficiently sensitive reporter system and an experimental design with paired samples.

Effect of intracellular pH on mutagenesis

Finally, we tested whether experimental perturbation of intracellular pH could affect mutation frequencies. We deleted two genes encoding subunits of the vacuolar H^+-ATPase, namely *vma2* and *vma3* (48). When cultured in media with 2% glucose at 23°C, ANOVA found a statistically significant difference among the three tested genotypes (P-value = 0.0182, see Figure 3C), although the Tukey HSD test showed that only the *vma3* vs. VMA^+ (i.e., ySR127 parental control) pairwise comparison had a statistically significant adjusted P-value (0.0137). Unfortunately, the two *vma* deletion backgrounds did not arrest properly in G_2 nor survive temperature shifting to 37°C, so it was not possible to collect those data.

We also used a pharmacological approach with a membrane permeabilizing compound called edelfosine, which causes intracellular acidification (49). Edelfosine treatment was compatible with reversible cell cycle arrest of *cdc13-1* cells. With 24-hour

exposure to 20 μM edelfosine at 37°C in media with 2% glucose, we observed a statistically significant increase in mutagenesis (paired t-test P-value = 0.000378, see Figure 3D). Again, with a sufficiently sensitive experimental system, it was possible to detect differences in mutation frequency by controlling a key parameter, intracellular pH.

Discussion

In this paper, we explored the mechanisms that contribute to a very common form of mutagenesis whose overall pattern resembles SBS signature 5 from COSMIC. Analogs of these similar mutational patterns are found in many biological systems (34). Given the ubiquitous nature of this set of related mutational patterns, we reasoned that the etiology is likely to be related to some endogenous process or agent that is well conserved, and that many biological systems are exposed to routinely. We previously tested whether deficiencies in molecular detoxification of endogenously generated reactive species caused increases in mutagenesis, but did not find such connections (34). Turning our attention to a less obvious candidate etiology, we eventually found that changing the carbon source metabolism of yeast cells did have large effects on SBS5-like mutagenesis. That set of results implicated the completion of glycolysis as an important requisite process for observing the SBS5-like mutagenesis (34). In this study, we ran additional experiments which consolidated and reaffirmed the results showing that glucose concentration is an important determinant of mutagenesis, while mitochondrial function is dispensable. Thinking about the product(s) of glycolysis that could contribute to the mutagenesis led us to investigating pH, since glycolysis is known to produce intracellular acidification (44,45).

A key factor in this study is the main experimental system that was used for most of the experiments. The *cdc13-1* ssDNA-based mutagenesis reporter system is very well suited for studying mutagenic effects that cannot be detected reliably using conventional mutagenesis reporter systems. When compared to conventional systems, where the reporter gene DNA is in double-stranded form, the ssDNA system is more sensitive to the

mutagenic effects of an experimental treatment, firstly because the nitrogenous bases are simply more exposed. In addition, DNA in a persistent single-stranded configuration (as opposed to transient ssDNA from melting of the duplex form) cannot benefit from high fidelity repair mechanisms that require a complementary strand. Without the potential intervention by DNA repair mechanisms, the ssDNA system can provide a purer readout of the effects of mutagenesis. Depending on the mutagen, the ssDNA reporter can be two to three orders of magnitude more sensitive than double-stranded DNA controls (35). Indeed, this system has been used successfully to elucidate the characteristics of multiple mutagens (35,37–40).

Early on in the various series of experiments, the high sensitivity of the ssDNA reporter and intracellular pH detection systems revealed to us that different yeast colonies used to grow biological replicate cultures can show considerable variance in baseline mutational frequency and pH values. To control for this apparently colony-intrinsic variance, we modified experiments to utilize paired designs whenever possible, i.e., the same colony was suspended in a small volume of water and then aliquoted equally to inoculate a pair of cultures with different experimental conditions. Using the paired experimental designs, we were able to leverage the high sensitivity of the mutagenesis and pH detection systems to best advantage.

We measured pH values when cells were metabolizing media with either 2% or 8% glucose. Determining extracellular (i.e., media) pH values was most straightforward, and showed that cells metabolizing more glucose produced more acidic conditioned media. This is as expected, since many of the excess protons from glycolysis would have to be extruded into the media, lowering its pH. We also found that the superfolder

pHluorin pH-sensitive GFP reporter was sufficiently sensitive to detect a significantly lower intracellular pH when cells metabolized 8% glucose. Since pH is on a logarithmic scale, the measured difference translated to about a two-fold increase in the numbers of protons in solution within cells. These results show that differences in pH due to different metabolic states can be measurable, in spite of the mechanisms for maintaining intracellular pH within a relatively narrow homeostatic range, which function specifically to counteract large shifts in pH within cells (47).

Our results also implicated pH as an important factor in the SBS5-like mutagenesis. Treatment with the membrane permeabilizing drug edelfosine caused intracellular acidification (49) and a significant increase in mutagenesis at 37°C, while metabolizing media with 2% glucose. Similarly, deletion of *vma3* deprived cells of a mechanism for regulating intracellular pH (48), and resulted in increased mutagenesis at 23°C in 2% glucose media. Deletion of *vma2* showed a similar trend, although not statistically different vs. ySR127 (VMA^+) controls by the Tukey HSD test. Neither *vma* mutant was able to tolerate the temperature shift to 37°C, likely because they couldn't cope with that stressor without a functional vacuole. Nonetheless, these results did point to measurable differences in mutation frequency when intracellular pH was perturbed. In addition, the ssDNA reporter system was sufficiently sensitive to detect a small, but statistically significant change in mutation frequency when extracellular pH was varied. Tukey HSD analysis showed that the significant pairwise differences were between pH 4 vs. pH 7 and between pH 5 vs. pH 7. Another way of interpreting this result is that neutral extracellular pH had an inhibitory effect on mutagenesis.

We propose that excess protons from glycolysis make a plausible candidate as a ubiquitous endogenous mutagen in effect, since the protons are produced constantly as a natural by-product of metabolism, can diffuse freely into the nucleus, and can react readily with DNA bases. The nucleus itself does not have mechanisms to regulate pH, so cytosolic acidification would also result in nuclear acidification (50). Protonation of nitrogenous bases can change their base pairing characteristics, as has been shown for protonation of adenine, cytosine, and thymine at their most likely predicted atomic positions (22). Biophysical experiments have shown that protonation at N1 of adenine and N3 of cytosine were especially prevalent in ssDNA, as these atoms would normally be protected by base pairing in dsDNA (51). In addition, three research groups have shown that protonation of adenine had the effect of stabilizing A^+:C wobble base pairs especially (52–54). This is a particularly intriguing connection, since the C > T and T > C transition mutations (which are most common in SBS5 and related mutational patterns) both can arise from the A^+:C wobble mispairs. We propose a model whereby protonation of bases in ssDNA increases the likelihood of impeding DNA re-synthesis by a high-fidelity replicative polymerase, which in turn increases the likelihood of recruitment of the error-prone translesion DNA synthesis machinery to extend past the mispairing, resulting in increased mutation frequency. Taken altogether, this work has shed new light on a common form of mutagenesis that is observed in a broad range of biological systems.

Materials and Methods

Reagents and Consumables

Bacto peptone (product code 211677) and yeast extract (212750) were purchased from Becton, Dickinson and Co. (Franklin Lakes, New Jersey). Canavanine (C9758), adenine sulfate dihydrate (AD0028), and digitonin (D141) were purchased from MilliporeSigma (St. Louis, Missouri). Agar (FB0010), glucose (GB0219), hygromycin (BS725), PCR purification spin column kit (BS654), plasmid DNA spin column kit (BS614), agarose (D0012), Tris-Borate-EDTA (TBE) buffer (A0026), ethidium bromide (D0197), sorbitol (SB0491), KH_2PO_4 (PBR0445), Na_2HPO_4 (S0404), NaCl (SB0476), 96-Well 2 mL Deep Plates (BR581-96NS), and amino acids or nucleotides (besides adenine) for media preparation were purchased from BioBasic (Markham, Ontario). KCl was purchased from Merck (Darmstadt, Germany). G418 sulfate (450-130) was purchased from Wisent (St-Bruno, Québec). Q5 DNA polymerase kit (M0491), T4 DNA ligase (M0202), XhoI (R0146), and XbaI (R0145) were purchased from New England Biolabs Canada (Whitby, Ontario). Microseals 'B' were purchased from Bio-Rad (Hercules, California). CELLSTAR black polystyrene clear bottom 96 well microtiter plates were purchased from Greiner Bio-One (Monroe, North Carolina). Phosphate buffered saline (PBS) was prepared as a 10× stock (pH 7.4) with the following components at these final concentrations: KH_2PO_4 (18 mM), Na_2HPO_4 (100 mM), NaCl (1.37 M), and KCl (27 mM). Plasmid p426MET25_sfpHluorin (MRV55) was purchased from Addgene (Watertown, Massachusetts). DH5α *E. coli* competent cells (18265-017) were purchased from Invitrogen (Waltham, Massachusetts).

Yeast Media

Routine culturing was done on YPDA rich solid media (2% Bacto peptone, 1% Bacto yeast extract, 2% glucose, supplemented with 0.001% adenine sulfate, 2% agar) or YPDA liquid rich media (2% Bacto peptone, 1% Bacto yeast extract, 2% glucose, supplemented with 0.001% adenine sulfate), as appropriate. Liquid rich media with 8% glucose (YPD8A) were same as baseline YPDA, except containing 8% glucose. Similarly, for YPDA with 6% sorbitol. Percentage values all refer to weight by volume (w/v).

For synthetic complete solid media, 1 L consisted of: 20 g agar, 20 g D-glucose, 5 g ammonium sulfate, 1.7 g yeast nitrogen base without amino acids or ammonium sulfate, 60 mg adenine sulfate, 50 mg L-arginine HCl, 75 mg L-aspartic acid, 100 mg L-glutamic acid, 20 mg L-histidine HCl, 50 mg L-isoleucine, 100 mg L-leucine, 120 mg L-lysine HCl, 20 mg L-methionine, 50 mg L-phenylalanine, 375 mg L-serine, 100 mg L-threonine, 50 mg L-tryptophan, 50 mg L-tyrosine, 150 mg L-valine, 60 mg uracil, and deionized water to 1 L total volume. pH was adjusted to 5.8 before autoclaving.

For canavanine media with low (0.33×) adenine, 1 L consisted of: 20 g agar, 20 g D-glucose, 5 g ammonium sulfate, 1.7 g yeast nitrogen base without amino acids or ammonium sulfate, 20 mg adenine sulfate, 75 mg L-aspartic acid, 100 mg L-glutamic acid, 20 mg L-histidine HCl, 50 mg L-isoleucine, 100 mg L-leucine, 120 mg L-lysine HCl, 20 mg L-methionine, 50 mg L-phenylalanine, 375 mg L-serine, 100 mg L-threonine, 50 mg L-tryptophan, 50 mg L-tyrosine, 150 mg L-valine, 60 mg uracil, and deionized water to 1 L total volume. pH was adjusted to 5.8 before autoclaving. After

cooling media to ≤ 60°C, 6 mL of 1% canavanine sulfate solution (filter sterilized) was added and stirred thoroughly to mix (before pouring the plates).

Yeast Genetics

The ySR127 yeast strain (a *MATα* haploid bearing the *cdc13-1* temperature sensitive allele (36,55)) and its derivatives were used in this study. ySR127 is itself derived from strain CG379 (56) and has a cassette of three reporter genes (*CAN1*, *URA3*, and *ADE2*) near the de novo left telomere of chromosome V. These three genes had been deleted from their native loci. Additional details about ySR127 were described previously (35). All strains are listed in Table 1 and available upon request.

vma2::HYG and *vma3::G418* derivatives of ySR127 were constructed by one step gene replacement using the respective antibiotic resistance marker (57). Constructions were verified by diagnostic replica plating and PCRs.

ρ^- petites were isolated from the ySR127 parental background as follows: Four ySR127 colonies were inoculated separately into YPDA liquid media and grown for three days at 23°C. 200 cells were plated onto YPDA solid media in five-fold replicate from each culture. In total, 1000 cells were screened from each culture. Plates were incubated at 23°C for five days. ρ^- candidates were selected based on small colony size, patched onto fresh YPDA, and tested by replica plating onto glycerol media.

ρ^0 petites were isolated from the ySR127 parental background as follows (58): Overnight cultures of ySR127 in YPDA were diluted 1:10 into fresh YPDA media with either 1 or 10 μg/mL ethidium bromide, and shaken at 23°C for three hours. Afterwards, cells were washed to remove the ethidium and 100 cells were plated onto YPDA from

each culture. ρ^0 candidates were selected based on small colony size, patched onto fresh YPDA, and tested by replica plating onto glycerol media.

To construct the pSG02 plasmid, the sfpHluorin gene was PCR-amplified from the p426MET25_sfpHluorin (MRV55) plasmid using primers that added XhoI and XbaI restriction sites. Purified PCR product and the pSG01 plasmid were digested with these enzymes to generate compatible sticky ends. Digested PCR product and plasmid were then ligated using T4 ligase. The ligation mix was then used to transform DH5α *E. coli* competent cells. Plasmid DNA was isolated from ampicillin-resistant clones using a miniprep kit, then screened by restriction digest to identify plasmids with the correct insertion. All steps were carried out according to manufacturer's instructions.

Mutation Frequency Assays

Mutagenesis experiments were initiated by inoculating single colonies separately into 5 mL of YPDA liquid rich media in round bottom glass tubes. For experiments comparing 2% vs. 8% glucose, each colony was suspended in a small volume of sterile water, then equal aliquots were inoculated into each media type. Cells were grown at 200 RPM in permissive temperature (23°C) for three days. Then, cultures were diluted ten-fold into fresh media in fresh glass tubes, shifted to restrictive temperature (37°C), and shaken gently at 150 RPM for 24 hours. When mutagenesis treatment was complete, cells were collected, lightly centrifuged, washed in water, and plated onto synthetic complete media to assess survival and onto canavanine-containing media with 0.33× adenine to select for mutants (Can^R colonies were off-white while Can^R Ade^- colonies turned red or pink). Care was taken to handle cells gently, as they were quite fragile after

temperature shift. Further details of this plating procedure were described previously in (59). The synthetic complete and canavanine plates were incubated at 23°C for five days. Plates were then imaged by scanner and colonies were counted using the Colony Counter plugin (60) for ImageJ (61).

Fluctuation Assays

Mutation rates were determined using fluctuation assays adapted from (62). Colonies were grown for 72 hours at 23°C in YPDA. Then, paired 10,000-fold dilutions were made using either YPDA (2% glucose) or YPD8A (8% glucose). 200 µL from each 10,000-fold dilution was put into a well of a 96-well 2 mL deep plate. Plates were covered securely with Microseal 'B' film and shaken for 72 hours at 23°C. Six cultures were selected at random from each test condition for determining cell titers using a hemacytometer and appropriate dilutions were plated on synthetic complete to assess plating efficiency. The rest of the cultures were plated onto canavanine media to identify mutants. To evaluate statistical differences in mutation rates, the flan.test() function from the flan package (version 0.9) (63) was applied, using default parameters (Luria-Delbrück distribution, maximum likelihood model). This parametric statistical test is essentially analogous to running a t-test (63).

Extracellular pH Measurements

pH of aliquots of conditioned culture media were determined using a pH meter (model number 860031) from Sper Scientific (Scottsdale, Arizona).

Intracellular pH Measurements

A superfolder pHluorin from (46) was used to measure intracellular pH. The calibration curve and the measurements were performed similarly to the protocol in (64). Briefly, to generate the calibration curves, cultures were incubated for 24 hours in YPDA or YPD8A media, centrifuged for 5 minutes at 4000 RPM, resuspended in PBS containing 100 mg digitonin, and incubated on room temperature for 10 minutes. Cells then were washed with PBS and put on ice. Next, cells were suspended to obtain an OD600 of 0.5 in PBS buffer of pH values ranging from 3.5 to 9.0 and transferred to CELLSTAR black polystyrene clear bottom 96 well microtiter plates. Superfolder pHluorin fluorescence emission was measured at 506 nm using a Synergy H1 Multi-Mode Plate Reader (BioTek, Winooski, Vermont) providing excitation bands of 7 nm centred around 390 and 470 nm. To generate the calibration curve, we plotted the corresponding buffer pH against the ratio of 390 and 470 nm (R390/470). As a reference for background fluorescence, a parental culture (i.e., without plasmid) was always grown simultaneously with cultures carrying the pSG02 plasmid expressing the superfolder pHluorin. For the measurement of the cytosolic pH of the samples, cell suspensions were diluted to an appropriate OD600 (ranging between 0.5 to 1.0) with preconditioned media from each culture before measurements were taken at 390 and 470 nm.

Statistical Analyses

t-tests were performed using the t.test() function in base R (version 4.1.1) (65). Analysis of variance model fitting and Tukey Honest Significant Differences (HSD) tests were done using the aov() and TukeyHSD() functions from the stats package (version

4.1.1) of base R (65). Data were processed and visualizations were generated using the tidyverse packages (version 1.3.1) (66).

Author Contributions: Both authors contributed to the following: Conceptualization, Data Curation, Formal Analysis, Investigation, Methodology, Validation, Visualization, and Writing -- Review and Editing. S.P.G. also contributed Writing -- Original Draft Preparation. K.C. contributed Funding Acquisition and Supervision.

References

1. De Bont R, van Larebeke N. Endogenous DNA damage in humans: a review of quantitative data. Mutagenesis. 2004 May 1;19(3):169–85.
2. Irigaray P, Belpomme D. Basic properties and molecular mechanisms of exogenous chemical carcinogens. Carcinogenesis. 2010 Feb 1;31(2):135–48.
3. Ikehata H, Ono T. The Mechanisms of UV Mutagenesis. J Radiat Res (Tokyo). 2011 Mar 1;52(2):115–25.
4. Keszenman DJ, Kolodiuk L, Baulch JE. DNA damage in cells exhibiting radiation-induced genomic instability. Mutagenesis. 2015 May 1;30(3):451–8.
5. Tice RR, Setlow RB. DNA repair and replication in aging organisms and cells. In: Handbook of the Biology of Aging. New York: Van Nostrand Reinhold; 1985.
6. Saparbaev MK, Zharkov DO. Glycosylase Repair. In: Reference Module in Life Sciences [Internet]. Elsevier; 2017. Available from: http://www.sciencedirect.com/science/article/pii/B9780128096338064815
7. Greenblatt MS, Bennett WP, Hollstein M, Harris CC. Mutations in the p53 tumor suppressor gene: clues to cancer etiology and molecular pathogenesis. Cancer Res. 1994;54(18):4855–78.
8. Neddermann P, Gallinari P, Lettieri T, Schmid D, Truong O, Hsuan JJ, et al. Cloning and Expression of Human G/T Mismatch-specific Thymine-DNA Glycosylase. J Biol Chem. 1996 May 31;271(22):12767–74.
9. Sassa A, Kanemaru Y, Kamoshita N, Honma M, Yasui M. Mutagenic consequences of cytosine alterations site-specifically embedded in the human genome. Genes Environ. 2016 Sep 1;38(1):17.
10. Ames BN, Shigenaga MK, Hagen TM. Oxidants, antioxidants, and the degenerative diseases of aging. Proc Natl Acad Sci. 1993 Sep 1;90(17):7915.
11. Helbock HJ, Beckman KB, Shigenaga MK, Walter PB, Woodall AA, Yeo HC, et al. DNA oxidation matters: the HPLC-electrochemical detection assay of 8-oxo-deoxyguanosine and 8-oxo-guanine. Proc Natl Acad Sci U S A. 1998 Jan 6;95(1):288–93.
12. Kadlubar FF, Anderson KE, Häussermann S, Lang NP, Barone GW, Thompson PA, et al. Comparison of DNA adduct levels associated with oxidative stress in human pancreas. Mutat Res Mol Mech Mutagen. 1998 Sep 20;405(2):125–33.
13. VanderVeen LA, Hashim MF, Shyr Y, Marnett LJ. Induction of frameshift and base pair substitution mutations by the major DNA adduct of the endogenous carcinogen malondialdehyde. Proc Natl Acad Sci. 2003 Nov 25;100(24):14247.
14. Lindahl T, Nyberg B. Rate of depurination of native deoxyribonucleic acid. Biochemistry. 1972 Sep 12;11(19):3610–8.
15. Lindahl T. Instability and decay of the primary structure of DNA. Nature. 1993 Apr 22;362(6422):709–15.
16. Nakamura J, Walker VE, Upton PB, Chiang SY, Kow YW, Swenberg JA. Highly Sensitive Apurinic/Apyrimidinic Site Assay Can Detect Spontaneous and Chemically Induced Depurination under Physiological Conditions. Cancer Res. 1998 Jan 15;58(2):222.
17. Haber JE. DNA recombination: the replication connection. Trends Biochem Sci. 1999 Jul 1;24(7):271–5.

18. Vilenchik MM, Knudson AG. Endogenous DNA double-strand breaks: Production, fidelity of repair, and induction of cancer. Proc Natl Acad Sci. 2003 Oct 28;100(22):12871.
19. Letouzé E, Shinde J, Renault V, Couchy G, Blanc JF, Tubacher E, et al. Mutational signatures reveal the dynamic interplay of risk factors and cellular processes during liver tumorigenesis. Nat Commun. 2017 Nov 3;8(1):1315.
20. Moriya M, Slade N, Brdar B, Medverec Z, Tomic K, Jelaković B, et al. TP53 Mutational signature for aristolochic acid: an environmental carcinogen. Int J Cancer. 2011 Mar 16;129(6):1532–6.
21. Alexandrov LB, Ju YS, Haase K, Van Loo P, Martincorena I, Nik-Zainal S, et al. Mutational signatures associated with tobacco smoking in human cancer. Science. 2016 Nov 4;354(6312):618.
22. Russo N, Toscano M, Grand A, Jolibois F. Protonation of thymine, cytosine, adenine, and guanine DNA nucleic acid bases: Theoretical investigation into the framework of density functional theory. J Comput Chem. 1998 Jul 15;19(9):989–1000.
23. Podolyan Y, Gorb L, Leszczynski J. Protonation of Nucleic Acid Bases. A Comprehensive Post-Hartree−Fock Study of the Energetics and Proton Affinities. J Phys Chem A. 2000 Aug 1;104(31):7346–52.
24. Masoodi HR, Bagheri S, Abareghi M. The effects of tautomerization and protonation on the adenine–cytosine mismatches: a density functional theory study. J Biomol Struct Dyn. 2016 Jun 2;34(6):1143–55.
25. Kimsey IJ, Szymanski ES, Zahurancik WJ, Shakya A, Xue Y, Chu CC, et al. Dynamic basis for dG•dT misincorporation via tautomerization and ionization. Nature. 2018 Jan 31;554:195.
26. Alberts B, Johnson A, Lewis J, Raff M, Roberts K, Walter P. DNA, Chromosomes and Genomes. In: Molecular Biology of the Cell. 6th ed. New York: W.W. Norton & Co.; 2014.
27. Alexandrov LB, Kim J, Haradhvala NJ, Huang MN, Tian Ng AW, Wu Y, et al. The repertoire of mutational signatures in human cancer. Nature. 2020 Feb 1;578(7793):94–101.
28. Alexandrov LB, Nik-Zainal S, Wedge DC, Campbell PJ, Stratton MR. Deciphering Signatures of Mutational Processes Operative in Human Cancer. Cell Rep. 2013 Jan 31;3(1):246–59.
29. COSMIC | SBS - Mutational Signatures [Internet]. [cited 2022 Jun 2]. Available from: https://cancer.sanger.ac.uk/signatures/sbs/
30. Alexandrov LB, Jones PH, Wedge DC, Sale JE, Campbell PJ, Nik-Zainal S, et al. Clock-like mutational processes in human somatic cells. Nat Genet. 2015 Nov 9;47:1402.
31. Ju YS, Martincorena I, Gerstung M, Petljak M, Alexandrov LB, Rahbari R, et al. Somatic mutations reveal asymmetric cellular dynamics in the early human embryo. Nature. 2017 Mar 22;543:714.
32. Rahbari R, Wuster A, Lindsay SJ, Hardwick RJ, Alexandrov LB, Al Turki S, et al. Timing, rates and spectra of human germline mutation. Nat Genet. 2015 Dec 14;48:126.
33. Dentro SC, Leshchiner I, Haase K, Tarabichi M, Wintersinger J, Deshwar AG, et al. Characterizing genetic intra-tumor heterogeneity across 2,658 human cancer genomes. Cell. 2021 Apr 15;184(8):2239-2254.e39.

34. Gelova SP, Doherty KN, Alasmar S, Chan K. Intrinsic base substitution patterns in diverse species reveal links to cancer and metabolism. bioRxiv. 2020 Jan 1;758540. (in revision).
35. Chan K, Sterling JF, Roberts SA, Bhagwat AS, Resnick MA, Gordenin DA. Base Damage within Single-Strand DNA Underlies In Vivo Hypermutability Induced by a Ubiquitous Environmental Agent. PLoS Genet. 2012 Dec 13;8(12):e1003149.
36. Garvik B, Carson M, Hartwell L. Single-stranded DNA arising at telomeres in cdc13 mutants may constitute a specific signal for the RAD9 checkpoint. Mol Cell Biol. 1995 Nov 1;15(11):6128–38.
37. Chan K, Resnick MA, Gordenin DA. The choice of nucleotide inserted opposite abasic sites formed within chromosomal DNA reveals the polymerase activities participating in translesion DNA synthesis. DNA Repair. 2013 Nov;12(11):878–89.
38. Degtyareva NP, Heyburn L, Sterling J, Resnick MA, Gordenin DA, Doetsch PW. Oxidative stress-induced mutagenesis in single-strand DNA occurs primarily at cytosines and is DNA polymerase zeta-dependent only for adenines and guanines. Nucleic Acids Res. 2013 Oct 1;41(19):8995–9005.
39. Chan K, Roberts SA, Klimczak LJ, Sterling JF, Saini N, Malc EP, et al. An APOBEC3A hypermutation signature is distinguishable from the signature of background mutagenesis by APOBEC3B in human cancers. Nat Genet. 2015 Sep;47(9):1067–72.
40. Saini N, Sterling JF, Sakofsky CJ, Giacobone CK, Klimczak LJ, Burkholder AB, et al. Mutation signatures specific to DNA alkylating agents in yeast and cancers. Nucleic Acids Res [Internet]. 2020 Mar 5 [cited 2020 Jun 3];(gkaa150). Available from: https://doi.org/10.1093/nar/gkaa150
41. Gelova SP, Doherty KN, Alasmar S, Chan K. Intrinsic base substitution patterns in diverse species reveal links to cancer and metabolism. bioRxiv. 2020 Mar 12;758540. (in review).
42. Nick McElhinny SA, Gordenin DA, Stith CM, Burgers PMJ, Kunkel TA. Division of Labor at the Eukaryotic Replication Fork. Mol Cell. 2008 Apr 25;30(2):137–44.
43. Burke RL, Tekamp-Olson P, Najarian R. The isolation, characterization, and sequence of the pyruvate kinase gene of Saccharomyces cerevisiae. J Biol Chem. 1983 Feb 25;258(4):2193–201.
44. Pronk JT, Yde Steensma H, Van Dijken JP. Pyruvate Metabolism in Saccharomyces cerevisiae. Yeast. 1996 Dec 1;12(16):1607–33.
45. Tripp BC, Smith K, Ferry JG. Carbonic Anhydrase: New Insights for an Ancient Enzyme. J Biol Chem. 2001 Dec 28;276(52):48615–8.
46. Reifenrath M, Boles E. A superfolder variant of pH-sensitive pHluorin for in vivo pH measurements in the endoplasmic reticulum. Sci Rep. 2018 Aug 10;8(1):11985.
47. Orij R, Brul S, Smits GJ. Intracellular pH is a tightly controlled signal in yeast. Syst Biol Microorg. 2011 Oct 1;1810(10):933–44.
48. Forgac M. Structure and Properties of the Vacuolar (H+)-ATPases *. J Biol Chem. 1999 May 7;274(19):12951–4.
49. Czyz O, Bitew T, Cuesta-Marbán A, McMaster CR, Mollinedo F, Zaremberg V. Alteration of Plasma Membrane Organization by an Anticancer Lysophosphatidylcholine Analogue Induces Intracellular Acidification and Internalization of Plasma Membrane

Transporters in Yeast. J Biol Chem. 2013 Mar 22;288(12):8419–32.
50. Casey JR, Grinstein S, Orlowski J. Sensors and regulators of intracellular pH. Nat Rev Mol Cell Biol. 2010 Jan 1;11(1):50–61.
51. Williams MC, Wenner JR, Rouzina I, Bloomfield VA. Effect of pH on the Overstretching Transition of Double-Stranded DNA: Evidence of Force-Induced DNA Melting. Biophys J. 2001 Feb 1;80(2):874–81.
52. Brown T, Leonard GA, Booth ED, Kneale G. Influence of pH on the conformation and stability of mismatch base-pairs in DNA. J Mol Biol. 1990 Apr 5;212(3):437–40.
53. Allawi HT, SantaLucia J. Nearest-Neighbor Thermodynamics of Internal A·C Mismatches in DNA: Sequence Dependence and pH Effects. Biochemistry. 1998 Jun 1;37(26):9435–44.
54. Siegfried NA, O'Hare B, Bevilacqua PC. Driving Forces for Nucleic Acid pKa Shifting in an A+·C Wobble: Effects of Helix Position, Temperature, and Ionic Strength. Biochemistry. 2010 Apr 20;49(15):3225–36.
55. Hartwell LH, Mortimer RK, Culotti J, Culotti M. Genetic Control of the Cell Division Cycle in Yeast: V. Genetic Analysis of cdc Mutants. Genetics. 1973 Jun;74(2):267–86.
56. Morrison A, Bell JB, Kunkel TA, Sugino A. Eukaryotic DNA polymerase amino acid sequence required for 3' → 5' exonuclease activity. Proc Natl Acad Sci. 1991 Nov 1;88(21):9473–7.
57. Rothstein RJ. One-step gene disruption in yeast. In: Methods in Enzymology [Internet]. Academic Press; 1983. p. 202–11. Available from: http://www.sciencedirect.com/science/article/pii/0076687983010150
58. Goldring Elizabeth S., Grossman Lawrence I., Marmur Julius. Petite Mutation in Yeast. J Bacteriol. 1971 Jul 1;107(1):377–81.
59. Chan K. Molecular Genetic Characterization of Mutagenesis Using a Highly Sensitive Single-Stranded DNA Reporter System in Budding Yeast. In: Muzi-Falconi M, Brown GW, editors. Genome Instability: Methods and Protocols [Internet]. New York, NY: Springer New York; 2018. p. 33–42. Available from: https://doi.org/10.1007/978-1-4939-7306-4_4
60. Colony Counter [Internet]. [cited 2022 Jun 18]. Available from: https://imagej.nih.gov/ij/plugins/colony-counter.html
61. Schneider CA, Rasband WS, Eliceiri KW. NIH Image to ImageJ: 25 years of image analysis. Nat Methods. 2012 Jul;9(7):671–5.
62. Krašovec R, Richards H, Gomez G, Gifford DR, Mazoyer A, Knight CG. Measuring Microbial Mutation Rates with the Fluctuation Assay. United States; 2019.
63. Mazoyer A, Drouilhet R, Despréaux S, Ycart B. flan: An R Package for Inference on Mutation Models. R J. 2017;1(9):334–51.
64. Orij R, Postmus J, Ter Beek A, Brul S, Smits GJ. In vivo measurement of cytosolic and mitochondrial pH using a pH-sensitive GFP derivative in Saccharomyces cerevisiae reveals a relation between intracellular pH and growth. Vol. 155, Microbiology,. Microbiology Society,; 2009. p. 268–78.
65. R Core Team. R: The R Project for Statistical Computing [Internet]. [cited 2020 Mar 11]. Available from: https://www.r-project.org/
66. Wickham H, Averick M, Bryan J, Chang W, McGowan L, François R, et al.

Welcome to the tidyverse. J Open Source Softw. 2019 Nov 21;4(43):1686.
67. Roberts SA, Sterling J, Thompson C, Harris S, Mav D, Shah R, et al. Clustered Mutations in Yeast and in Human Cancers Can Arise from Damaged Long Single-Strand DNA Regions. Mol Cell. 2012 May 25;46(4):424–35.

1 **Figures**

2 Figure 1A

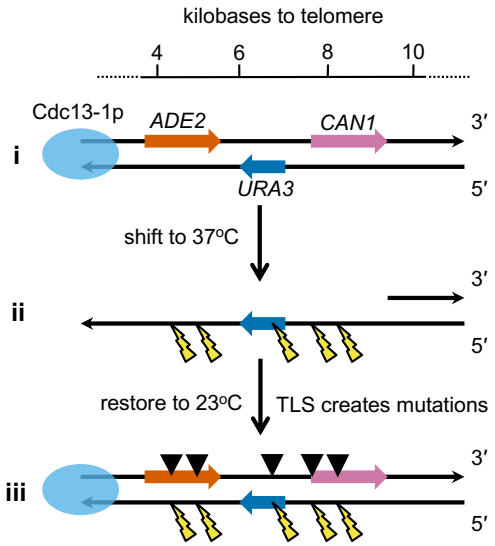

3

4 Figure 1B

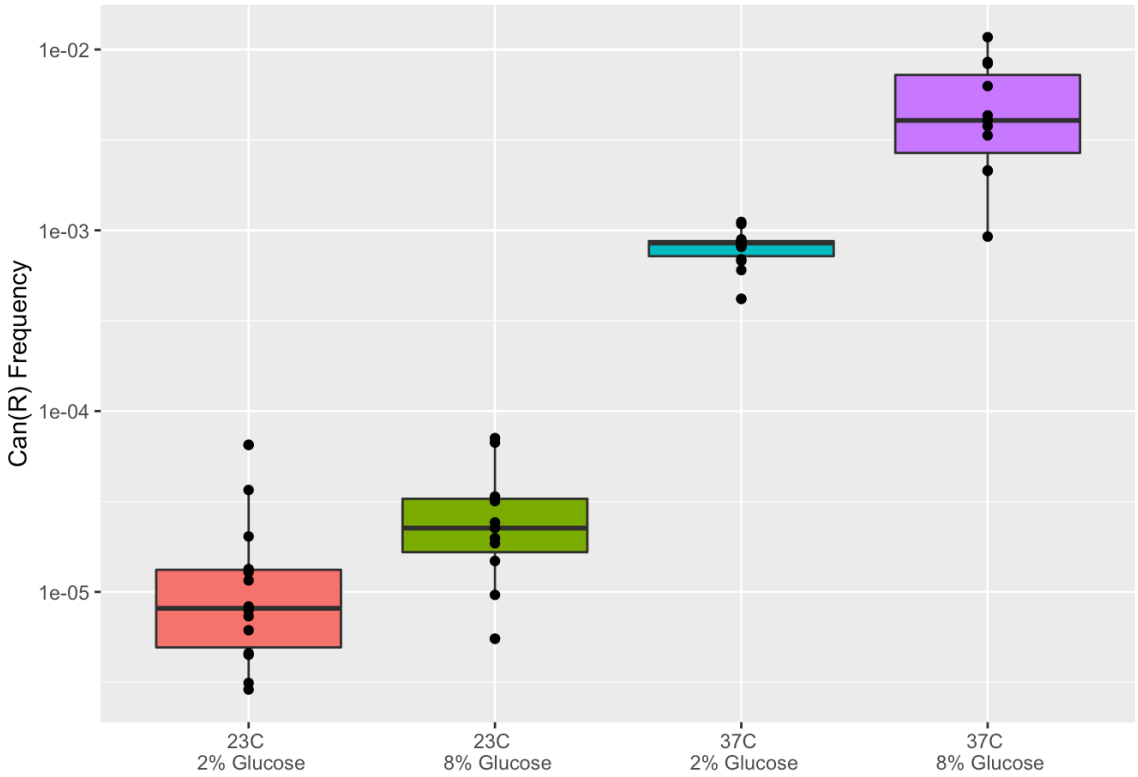

5

1 Figure 1C

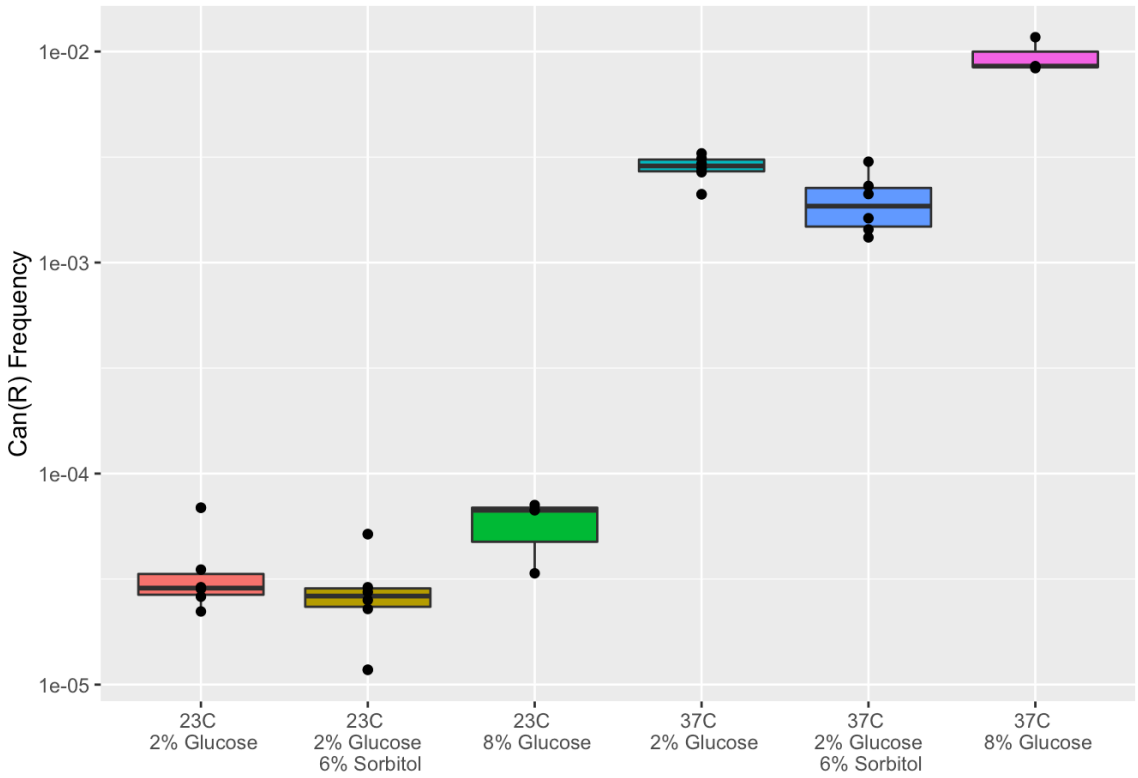

2

3

1 Figure 2A

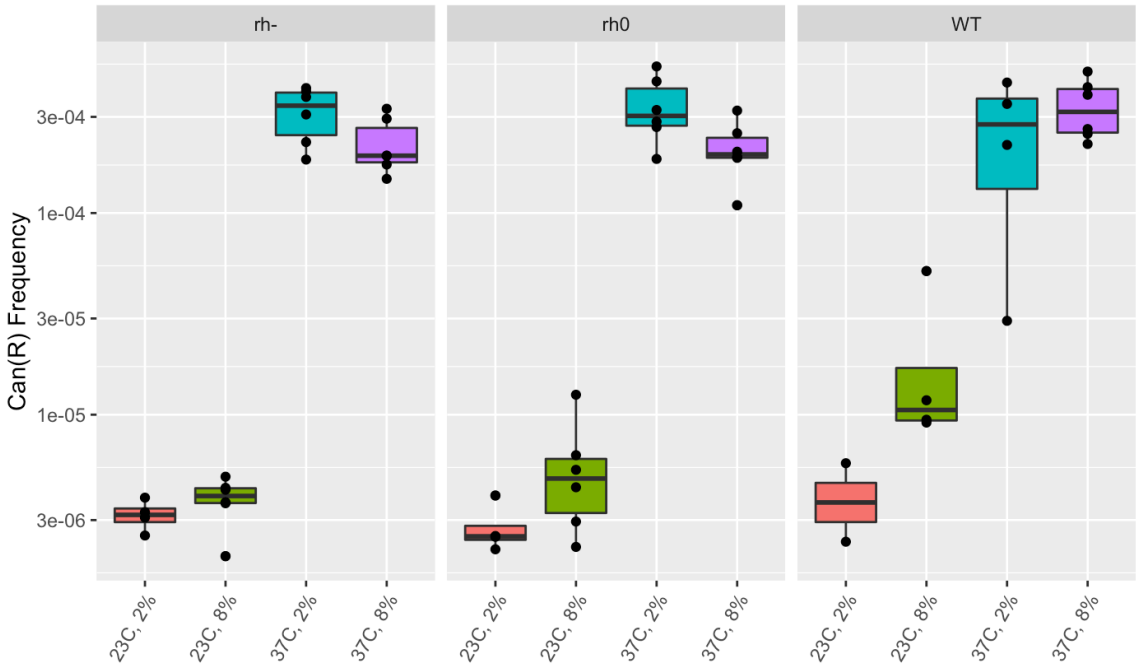

2

3 Figure 2B

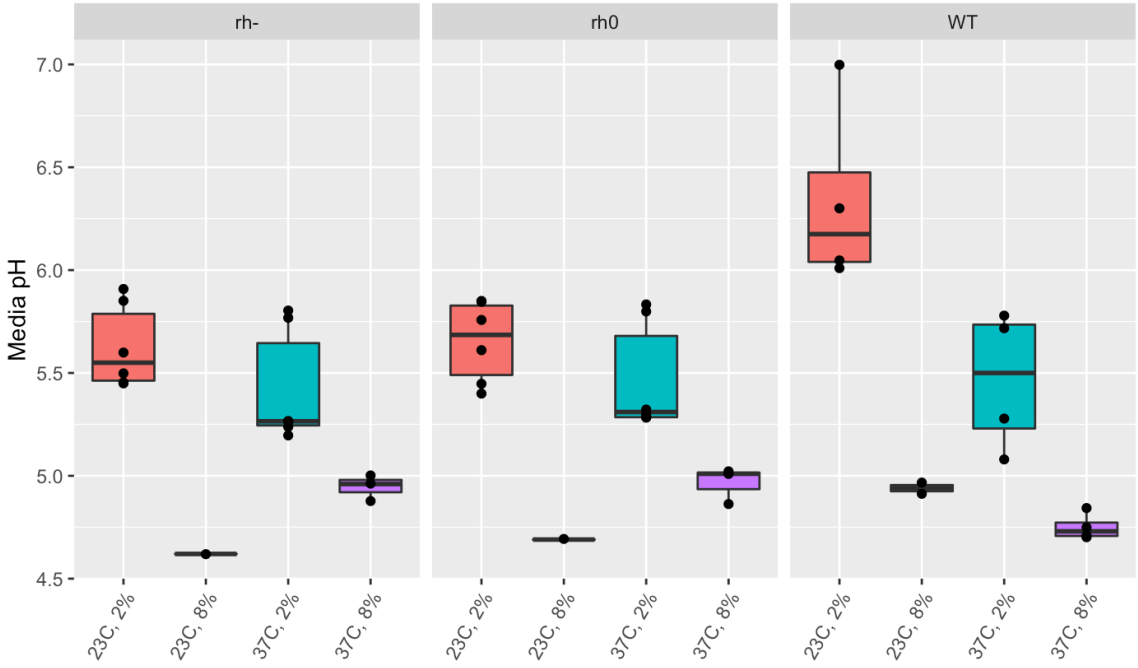

4

5

1 Figure 2C

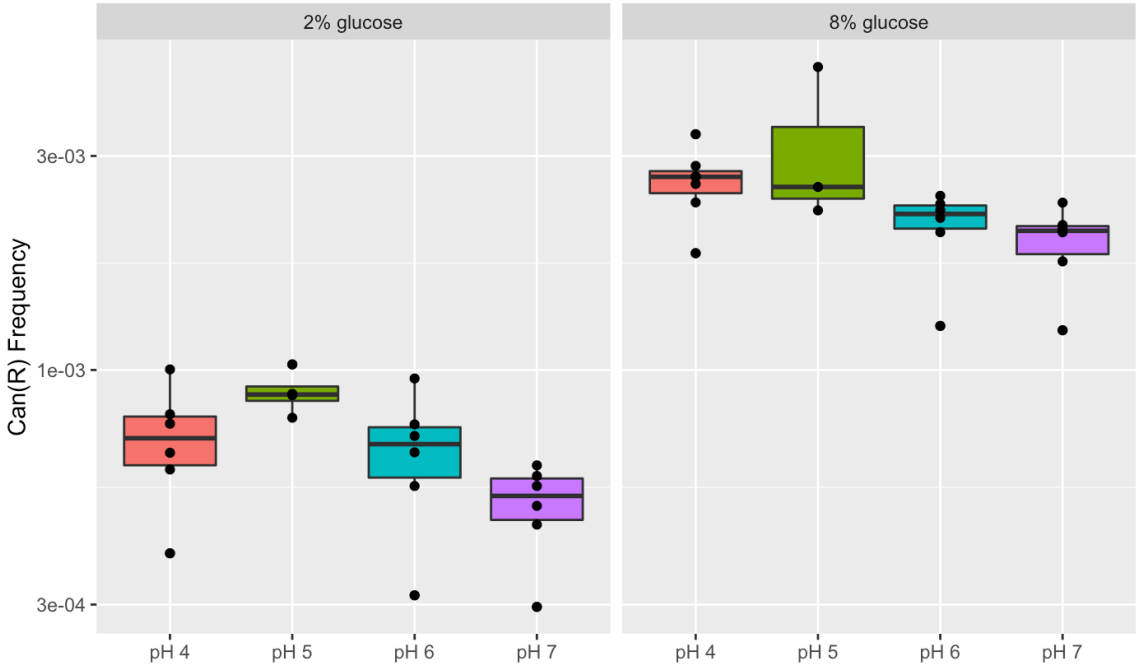

2

3

1 Figure 3A

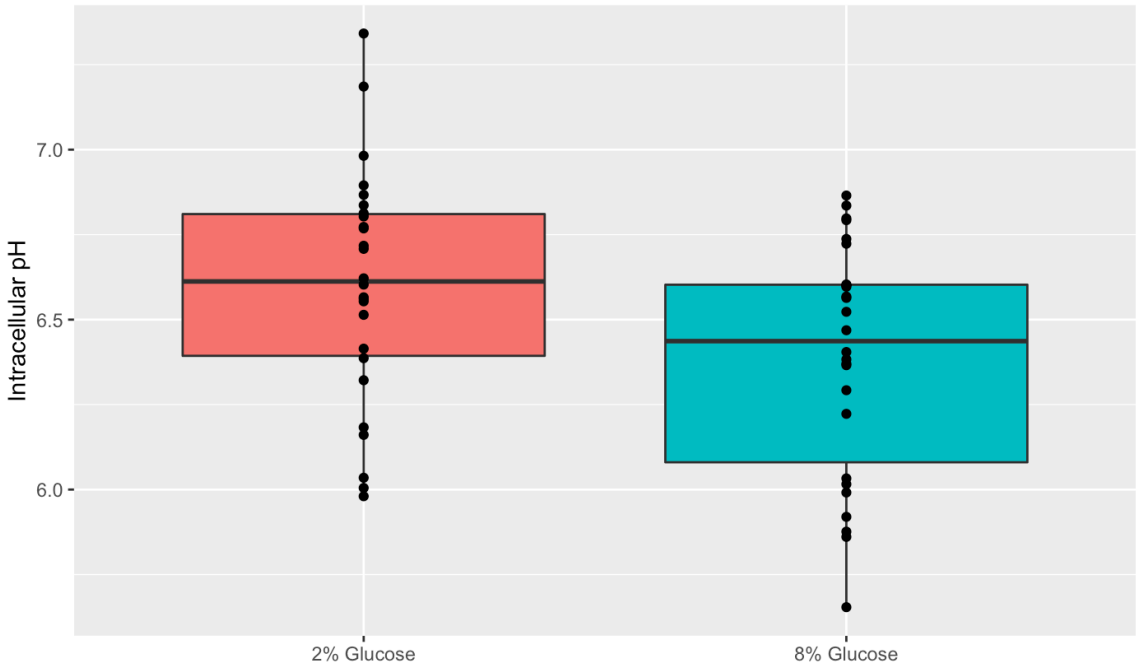

2

3 Figure 3B

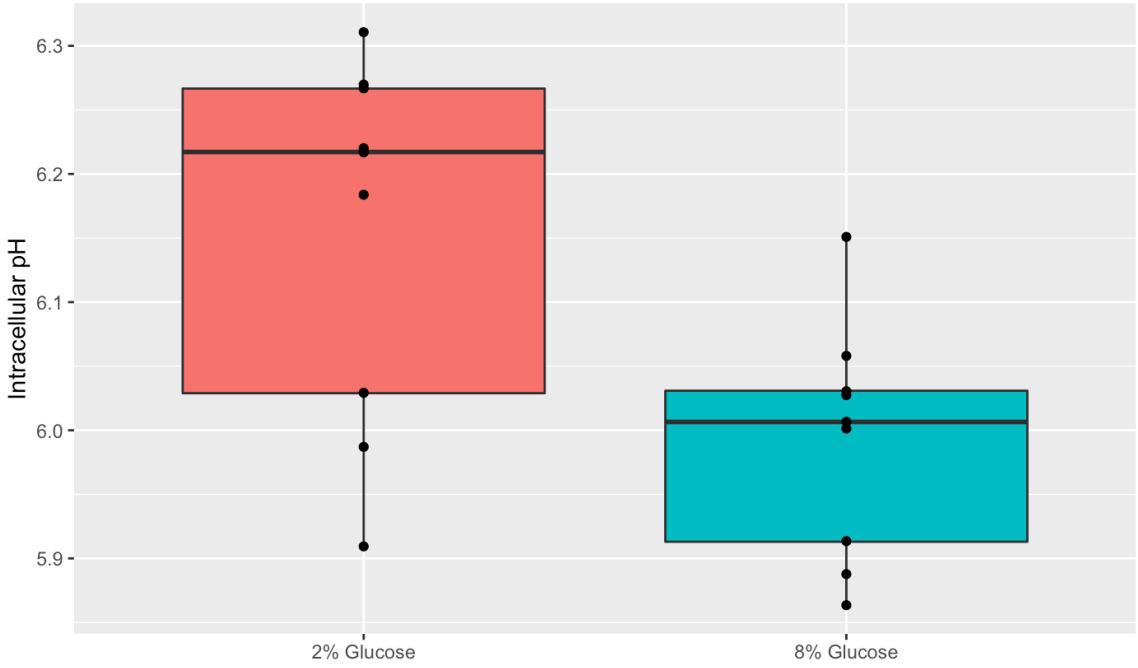

4

5

1 Figure 3C

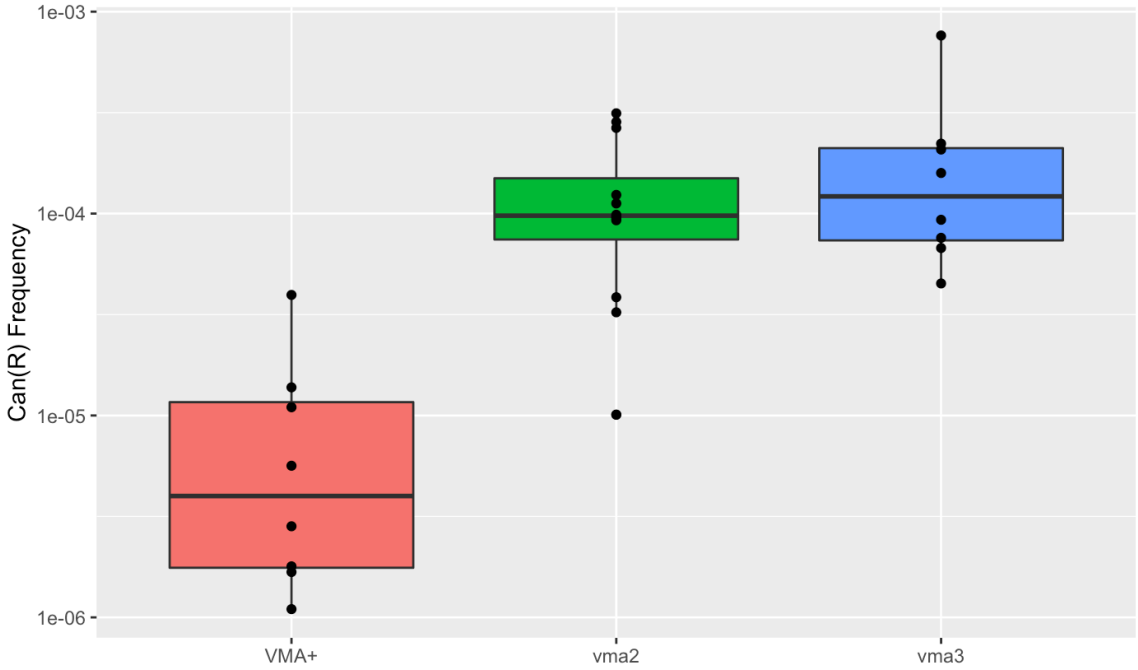

2

3 Figure 3D

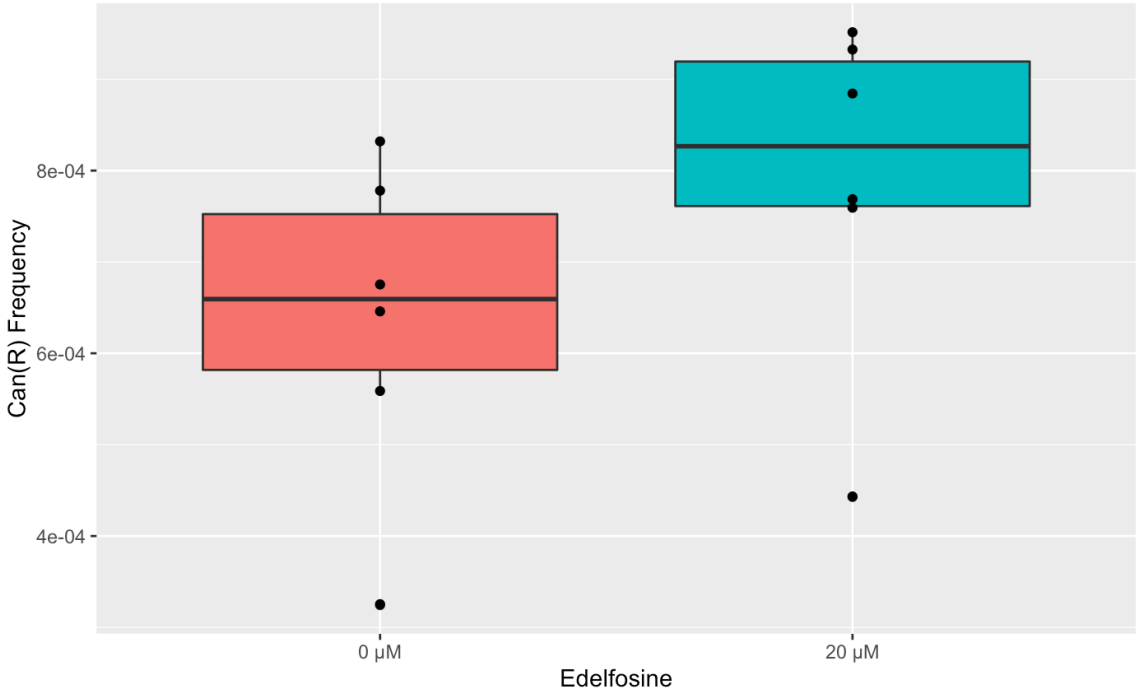

4

5

1 **Tables**

2 Table 1: List of yeast strains and plasmids used in this work.

Name	Genotype/Description	Reference
ySR127	*MATα cdc13-1 his7-2 leu2-3,112 trp1-289 lys2::CAN1-URA3-ADE2* (in left sub-telomeric region of chr. V)	(35)
ySR128	*MATα his7-2 leu2-3,112 trp1-289 lys2::CAN1-URA3-ADE2* (at ~345 kb from right telomere of chr. II)	(67)
yKC023	*MATα cdc13-1 his7-2 leu2-3,112 trp1-289 lys2::CAN1-URA3-ADE2* (at ~345 kb from right telomere of chr. II)	(35)
yKC005	*MATα his7-2 leu2-3,112 trp1-289 lys2::CAN1-URA3-ADE2* (in left sub-telomeric region of chr. V)	this study
yKC530, yKC531, yKC532	*MATα cdc13-1 his7-2 leu2-3,112 trp1-289 vma2::HYG lys2::CAN1-URA3-ADE2* (in left sub-telomeric region of chr. V)	this study
yKC536, yKC537	*MATα cdc13-1 his7-2 leu2-3,112 trp1-289 vma3::G418 lys2::CAN1-URA3-ADE2* (in left sub-telomeric region of chr. V)	this study
pSG01	p416 vector backbone with KanMX and Amp resistance markers	this study
pSG02	p416 vector backbone with KanMX and Amp resistance markers, and sfpHluorin insert under control of TEF1 promoter	this study

3

4 Table 2: Tukey HSD adjusted P-values for pairwise comparisons among media

5 containing 2% glucose, 2% glucose + 6% sorbitol, or 8% glucose.

Comparison	23°C	37°C
2% glucose vs. 2% glucose + 6% sorbitol	0.743	0.274
2% glucose vs. 8% glucose	0.171	0.0000007
2% glucose + 6% sorbitol vs. 8% glucose	0.0620	0.0000002

6

7

Table 3: Summary of data from fluctuation assays to determine mutation rates of the following strains while metabolizing media with either 2% or 8% glucose: ySR127 (*cdc13-1* with sub-telomeric reporter); ySR128 (*CDC*$^+$ with mid-chromosome reporter); yKC023 (*cdc13-1* with mid-chromosome reporter); and yKC005 (*CDC*$^+$ with sub-telomeric reporter).

Strain	Mutation Rate in 2% Glucose	Mutation Rate in 8% Glucose	flan.test Parametric Test P-value
ySR127	2.57×10^{-6}	6.60×10^{-6}	1.42×10^{-12}
ySR128	1.35×10^{-6}	1.80×10^{-6}	0.0111
yKC023	2.34×10^{-6}	2.48×10^{-6}	0.648
yKC005	8.93×10^{-7}	9.34×10^{-7}	0.804

Table 4: Tukey HSD adjusted P-values for pairwise comparisons of external pH among wild-type, ρ^-, and ρ^0 cells under different treatments.

Comparison	Adjusted P-value
WT vs. ρ^-	0.761
WT vs. ρ^0	0.921
ρ^- vs. ρ^0	0.941
23°C, 2% vs. 8% glucose	1.0×10^{-6}
37°C, 2% vs. 8% glucose	7.49×10^{-5}
2% glucose, 23°C vs. 37°C	5.78×10^{-3}
8% glucose, 23°C vs. 37°C	0.965

1 Table 5: Tukey HSD adjusted P-values for pairwise comparisons of mutation frequencies

2 in cells that were temperature shifted in media with different pH.

Comparison	Adjusted P-value
pH 4 vs. pH 5	0.918
pH 4 vs. pH 6	0.221
pH 4 vs. pH 7	0.0346
pH 5 vs. pH 6	0.120
pH 5 vs. pH 7	0.0221
pH 6 vs. pH 7	0.825

3

4

Figure Captions

Figure 1: Mutagenesis depends on sugar concentration in the media. (A) Schematic diagram of *cdc13-1* sub-telomeric triple reporter gene cassette system in strain ySR127 and its derivatives. (i) Three reporter genes, *CAN1*, *URA3*, and *ADE2*, were relocated from their native loci to the sub-telomeric region of a de novo telomere at the end of the left arm of chromosome V. The scale at the top indicates kilobases to beginning of telomeric repeats. (ii) Upon shifting to 37°C, the telomeric capping complex dissociates due to the mutant Cdc13-1 protein, exposing the chromosome end to enzymatic resection that generates long stretches of ssDNA. The long ssDNA triggers the DNA damage checkpoint to arrest cells in G_2. (iii) When cells are restored to 23°C, the DNA is restored to double-stranded form by re-synthesis of the complementary strand. Error-prone translesion synthesis polymerases can introduce mutations, which can be detected by selecting for inactivation of reporter genes. (B) Canavanine resistance (Can^R) frequencies of ySR127 cells at 23°C or after 24-hour shift to 37°C, metabolizing media with 2% or 8% glucose. (C) Can^R frequencies of ySR127 cells at 23°C or after 24-hour shift to 37°C, metabolizing media with 2% glucose, 2% glucose + 6% sorbitol, or 8% glucose.

Figure 2: Mutagenesis does not depend on mitochondrial function, but is linked to extracellular pH. (A) Can^R frequencies of ρ^-, ρ^0, and wild-type (ySR127) cells at 23°C or after 6-hour shift to 37°C, metabolizing media with 2% or 8% glucose. (B) Media (i.e., extracellular) pH of ρ^-, ρ^0, and wild-type cells at 23°C or after 6-hour shift to 37°C,

metabolizing media with 2% or 8% glucose. (C) Can^R frequencies of ySR127 cells after 24-hour shift to 37°C, metabolizing media with 2% glucose that was adjusted to the indicated pH values.

Figure 3: Glucose metabolism and mutagenesis are linked to intracellular pH. (A) Intracellular pH of ySR127 cells metabolizing media with 2% or 8% glucose at 23°C. (B) Intracellular pH of ySR127 cells metabolizing media with 2% or 8% glucose after 24-hour shift to 37°C. (C) Can^R frequencies of *vma2Δ*, *vma3Δ*, and wild-type (ySR127) cells at 23°C, metabolizing media with 2% glucose. (D) Can^R frequencies of ySR127 cells after 24-hour shift to 37°C, metabolizing media with 2% glucose and treated with either 0 or 20 μM edelfosine.

Supporting Information Caption

S1 Table: Tables of all numerical values used to generate graphs depicted in the figures.